Supplementary Information (SI) for Materials Advances.

SUPPORTING INFORMATION

Tunable slow photon effect and local surface plasmon in Ag-immobilized TiO_2 inverse opal films for enhancing pollutant photodegradation

Thi Kim Ngan Nguyen[a,*], Fabien Grasset[b], Satoshi Ishii[c], Hiroshi Fudouzi[d], Tetsuo Uchikoshi[b,d]

[a]International Center for Young Scientists, Global Networking Division, National Institute for Materials Science, 1-2-1 Sengen, Tsukuba, Ibaraki 305-0044, Japan

[b]CNRS–Saint-Gobain–NIMS, IRL3629, Laboratory for Innovative Key Materials and Structures, National Institute for Materials Science, 1-1 Namiki, Tsukuba, Ibaraki 305-0044, Japan

[c]Research Center for Materials Nanoarchitectonics (MANA), National Institute for Materials Science, 1-1 Namiki, Tsukuba, Ibaraki 305-0044, Japan

[d]Research Center for Electronic and Optical Materials, National Institute for Materials Science, 1-2-1 Sengen, Tsukuba, Ibaraki 305-0044, Japan

*Corresponding author: Thi Kim Ngan NGUYEN

Full postal address: International Center for Young Scientists, National Institute for Materials Science (NIMS), 1-2-1 Sengen, Tsukuba, Ibaraki 305-0047, Japan

E-Mail address: NGUYEN.Thikimngan@nims.go.jp

TABLES

Table S1. The calculation of stop band peak, fraction of air, and TiO_2 in inverse opal structure by using Bragg's law equation.

Sample	D (nm)	Testing λmax (nm)	f_{air}	f_{water}	f_{TiO2}
Opal	316	734	0.36		
IO(air)	250	474	0.94		0.06
IO (water) 90°	*250*	*460*		*0.94*	
IO (water) 5°		*438*		*0.94*	
Opal	338	818	0.30		
IO (air)	288	568	0.92		0.08
IO (water) 90°	*288*	*530*		*0.92*	
IO (water) 5°		*504*		*0.92*	
Opal	387	921	0.34		
IO (air)	318	613	0.93		0.07
IO (water) 90°	*318*	*585*		*0.93*	
IO (water) 5°		*556*		*0.93*	

Table. S2 The optical absorbance and indirect band gap of the disorder inverse opal TiO_2 introduced silver composites.

Samples	Absorbance peak (nm)	Absorbance range (nm)	Optical Eg (eV)
TiO_2		330-390	3.17
TiO_2 Ag1	450	389-620	2.19
TiO_2 Ag2	450	389-620	2.19
TiO_2 Ag3	450	392-620	2.19
TiO_2 Ag4	450	398-630	2.25
TiO_2 AgNS1	477	400-540	2.37
TiO_2 AgNS2	465	398-570	2.32
TiO_2 AgNS3	455	392-601	2.31
TiO_2 AgNS4	442	389-578	2.35

Table S3. The Ag and Ti atomic ratios assigned to NS-combined Ag and bare Ag at different positions inside the inverse opal wall were calculated by using STEM-EDX mapping.

Position*	TIO-AgNS4	TIO-Ag4
	(at.%Ag)10^{-3}/(at.%Ti)	
1	18.3	1.9
2	17.6	5.1
3	17.9	4.4
4	20.2	21.0
5	17.4	18.7
Ave.	18.3 ± 0.2	10.7 ± 1.5

Table S4. The atomic percentages of the elements existing in the composite films.

Films	C1s	O1s	Ti2p	Ag3d	S2p	Na1s
				% at.		
ITO250 Ag4	8.5	62.1	22.41	0.23	0	6.77
ITO250 AgNS4	19.4	52.8	17.20	1.41	0.66	8.59

Table S5. XPS binding energy (eV) analysis of TIO250 combined with Ag4 and AgNS4 NPs.

		TIO	TIO-Ag4	TIO-AgNS4	AgNS4
			Binding energy (eV)		
Ti	2p3/2	459.4	459.4	459.3	
	2p1/2	465.1	465.2	465.1	
O1s			530.1 (O-); 531.8 (S=O); 530.7 (Ti-O); 532.7 (O-H)	530.1 (O-); 531.8 (S=O); 530.7 (Ti-O); 532.7 (O-H)	530 (O-); 532 (S=O); 531.2 (O-H)
Ag3d	3d5/2		368.2 (Ag); 367.6 (Ag_2O) (Ag:Ag_2O = 0.26:1)	368.1 (Ag); 367.8 (Ag_2O) Ag:Ag2O = 14.5:1	368.1 (Ag); 367.8 (Ag_2O) Ag:Ag2O = 14.5:1
	3d3/2		374.2; 373.6	374.1 (Ag); 373.8 (Ag2O) (AgO/Ag2O)	374.1 (Ag); 373.8 (Ag2O) (AgO/Ag2O)

S2p	2p1/2	168.6	168.1 (C-SO3-)
	2p3/2	169.8	169.3
C1s		284.9 (C=C); 285.6 C-C); 286.4 (C-S);	283.5; 284.6 (C=C); 285.4 (C-C); 286.1 (C-S)

Table. S6. The calculated intensity of the absorbance of the disordered and ordered TIO deposited AgNS4 from Figure 7. The enhanced percentages were calculated by the normalized intensity when the highest peak was recorded at 450 nm.

Absorbance peak	TIO AgNS4 Powder		TIO288 AgNS4		TIO318 AgNS4	
	Real intensity	Normalized intensity	Real intensity	Normalized intensity	Real intensity	Normalized intensity
450	0.2336	1	0.206	1	0.17	1
480	0.185	0.791952	0.178266	0.865369	0.155	0.911765
510	0.1227	0.525257	0.11177	0.542573	0.109	0.641176
550	0.0259	0.110873	0.0348	0.168932	0.0189	0.111176

Table S7. The photocatalytic rate parameters of the TIO films without or with different Ag NPs.

Samples	Photodegradation rate after 1h (%)	Photodegradation Kinetic (10^3.min^{-1})	Photodegradation rate after 2h (%)	Photodegradation rate after 4 cycles (%)
TIO250	45.9	9.3		
TIO288	44.5	8.7	79.5	71.8
TIO318	40.7	7.8		
TIO250Ag4	60.7	13.2		
TIO288 Ag4	62.8	15.3	87.0	87.6
TIO318 Ag4	63.2	15.7		
TIO250 AgNS4	64.1	15.3		
TIO288 AgNS4	68.4	17.3	91.5	91.3
TIO318	65.8	15.9		

AgNS4

Table S8. The EIS parameter (Rct, Rs, Csc) was calculated from the Niquyst plots and ω_{max} was calculated from the Bode plots. The electron lifetime τ_n was calculated in association with the frequency maximum by the equation $\tau_n = 1/2\pi\omega_{max}$.

Samples	Rct (Ω)	Csc μF	Rs(Ω)	Rct (Ω × 10^4)	Csc μF	ω_{max} (Hz)	τ_n (ms) $1/2\pi\omega_{max}$
	Dark			illumination at angle of 90°			
TIO250	9.1×10^{13}	7.2	116.3	6.2	9.9	5.95	22.9
TIO288	2.8×10^{13}	7.2	93.7	11.6	9.7	5.5	26.8
TIO318	2.9×10^{13}	7.5	101.9	8.1	10.2	5.5	26.4
TIO250 Ag4	1.4×10^{6}	6.5	166.2	8.6	9.9	5.1	31.2
TIO288 Ag4	1.3×10^{6}	6.8	196.7	10.6	9.9	4.5	33.6
TIO318 Ag4	1.8×10^{6}	6.1	144.3	8.9	10.1	5.5	26.7
TIO250 AgNS4	3.8×10^{6}	6.3	203.8	10.2	8.7	3.8	36.4
TIO288 AgNS4	6.9×10^{6}	6.8	183.5	11.7	9.0	4.0	39.4
TIO318 AgNS4	6.8×10^{6}	6.1	200	13.6	8.1	3.7	39.3

FIGURES

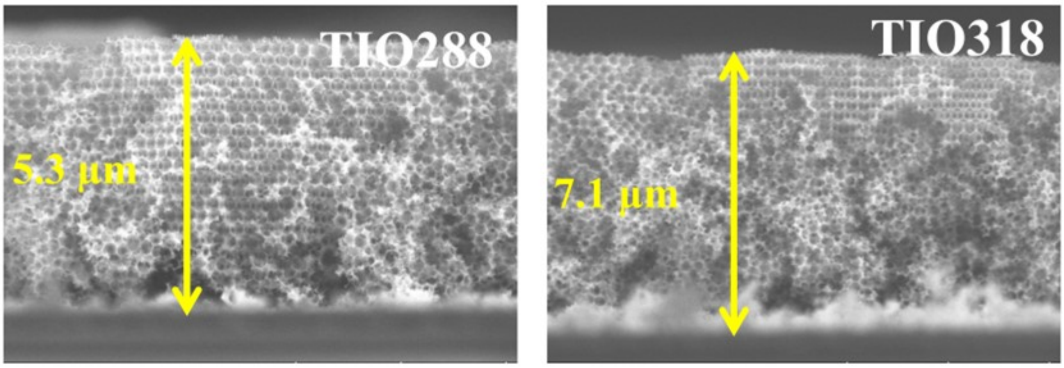

Figure S1. FE-SEM images of the cross-section view of TIO films.

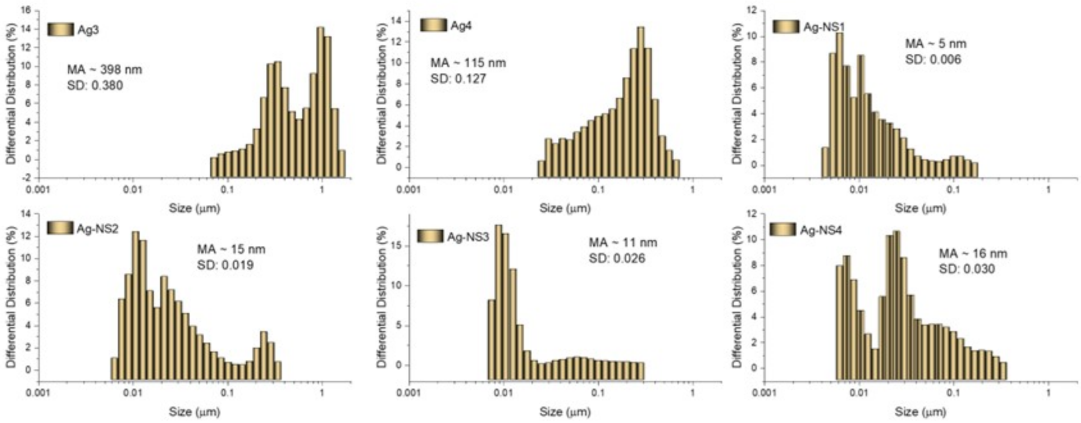

Figure S2. Differential distribution and size distributions of the Ag3, Ag4, Ag-NS1, Ag-NS2, Ag-NS3, and Ag-NS4 NPs after synthesizing for 1 hour.

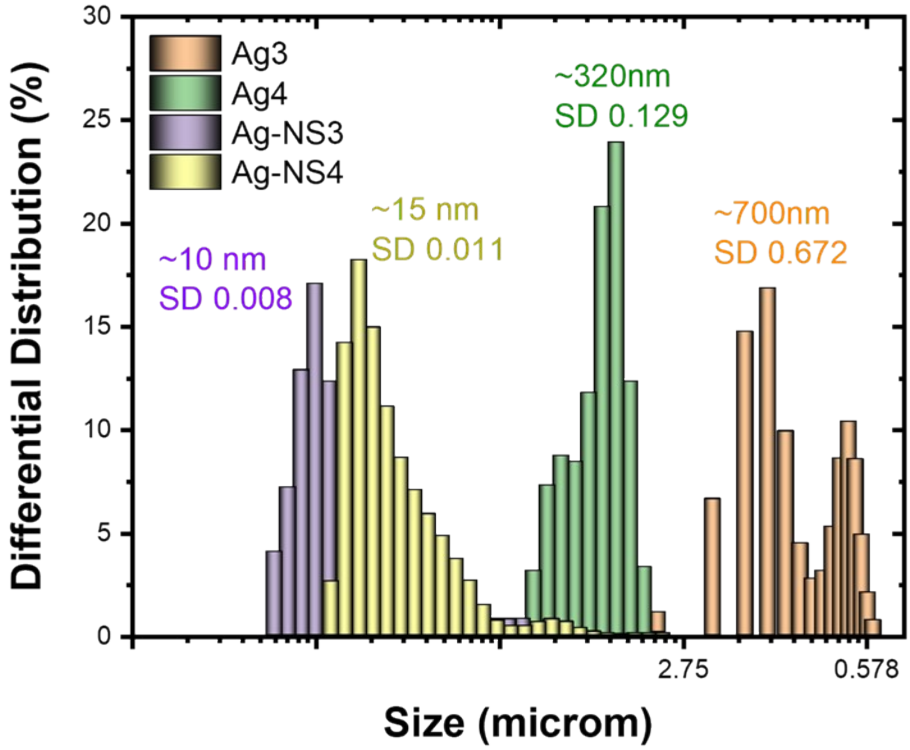

Figure S3. Differential distribution and size distributions of the Ag3, Ag4, Ag-NS3, and Ag-NS4 NPs after 2 months.

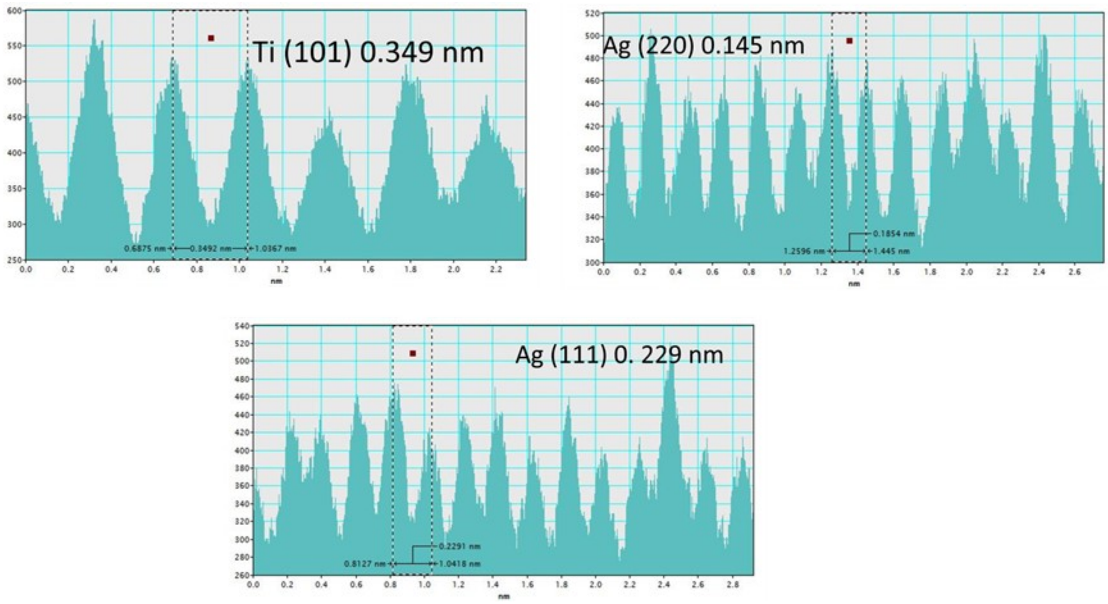

Figure S4. The calculated profile of the pattern of the AgNS4 NPs.

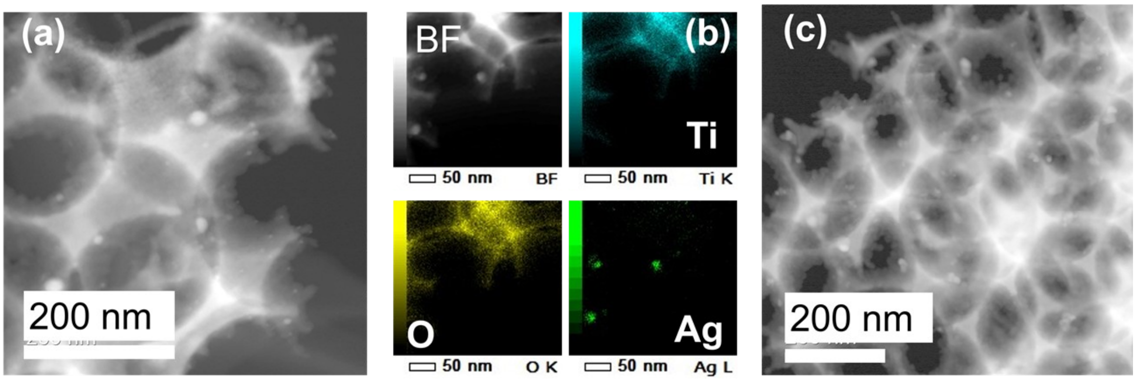

Figure S5. a) STEM, and b) EDX-STEM images of the TIO250 deposited AgNS4. c) STEM of the TIO250 deposited Ag4.

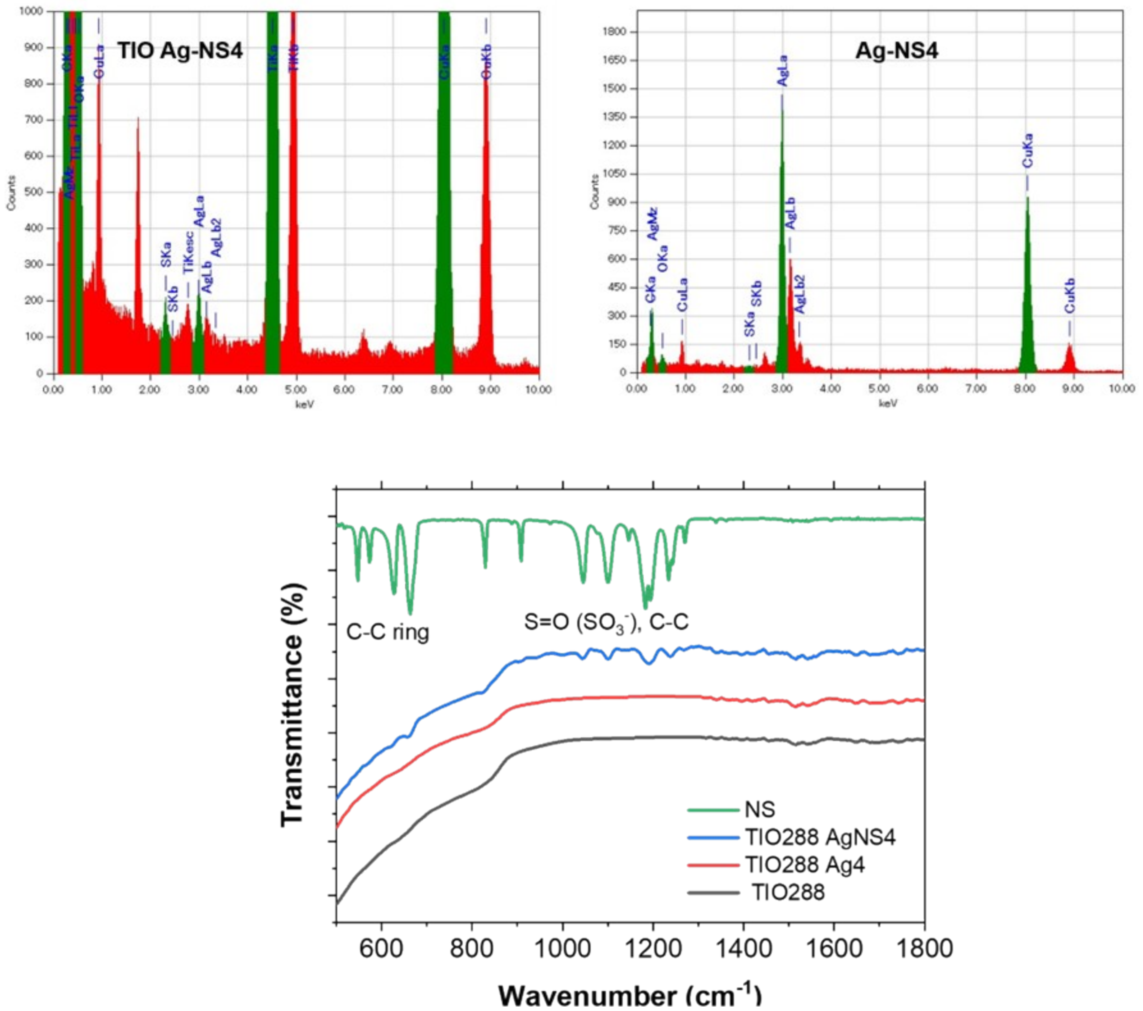

Figure S6. The element spectra measured by STEM-EDX mappings of the AgNS4 and TIO AgNS4 upper and the FT-IR spectra of the NS and TIO films.

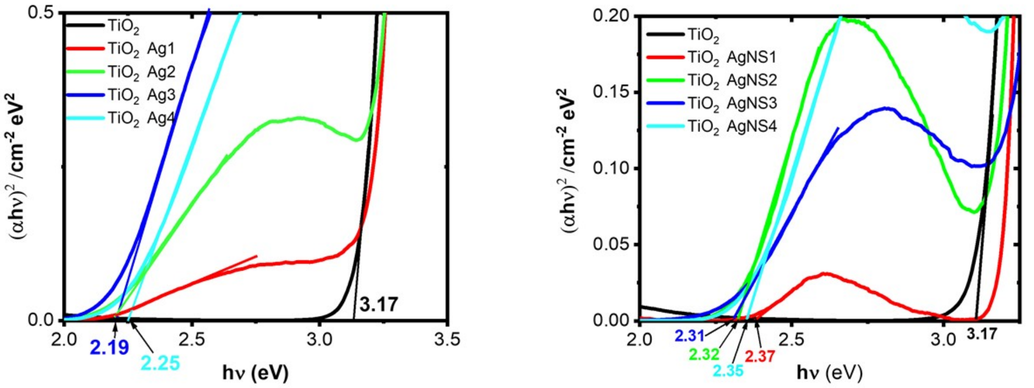

Figure S7. The Tauc plots calculated from absorbance spectra for estimating the optical energy gap.

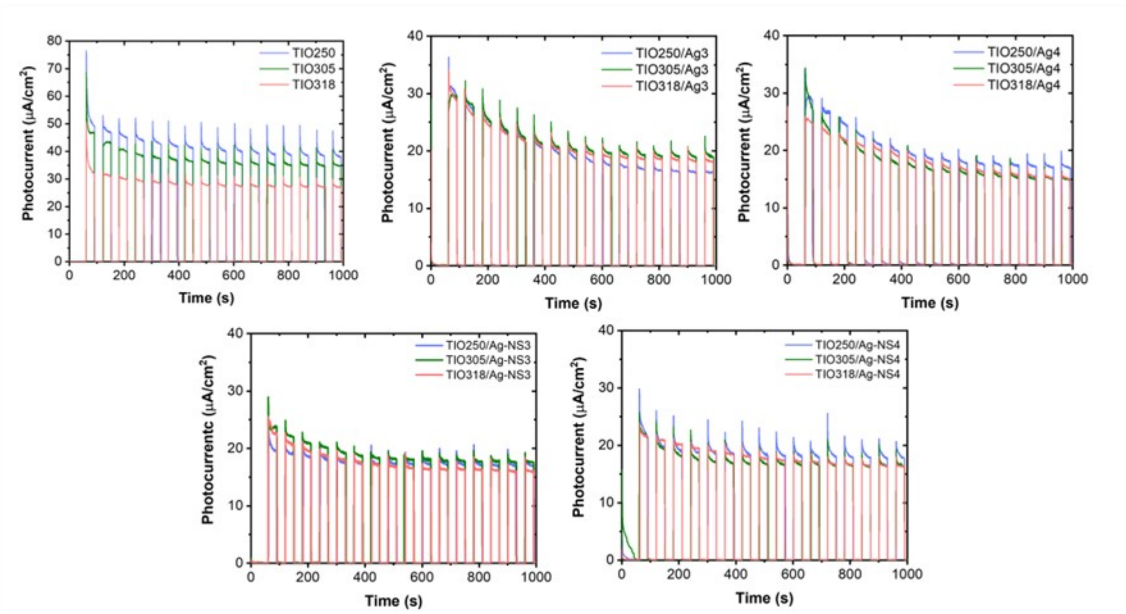

Figure S8. Reproducible on/off switching curves of the photocurrent of the TIOx (x = 250, 288, and 318) without and with the deposition of different Ag NPs.

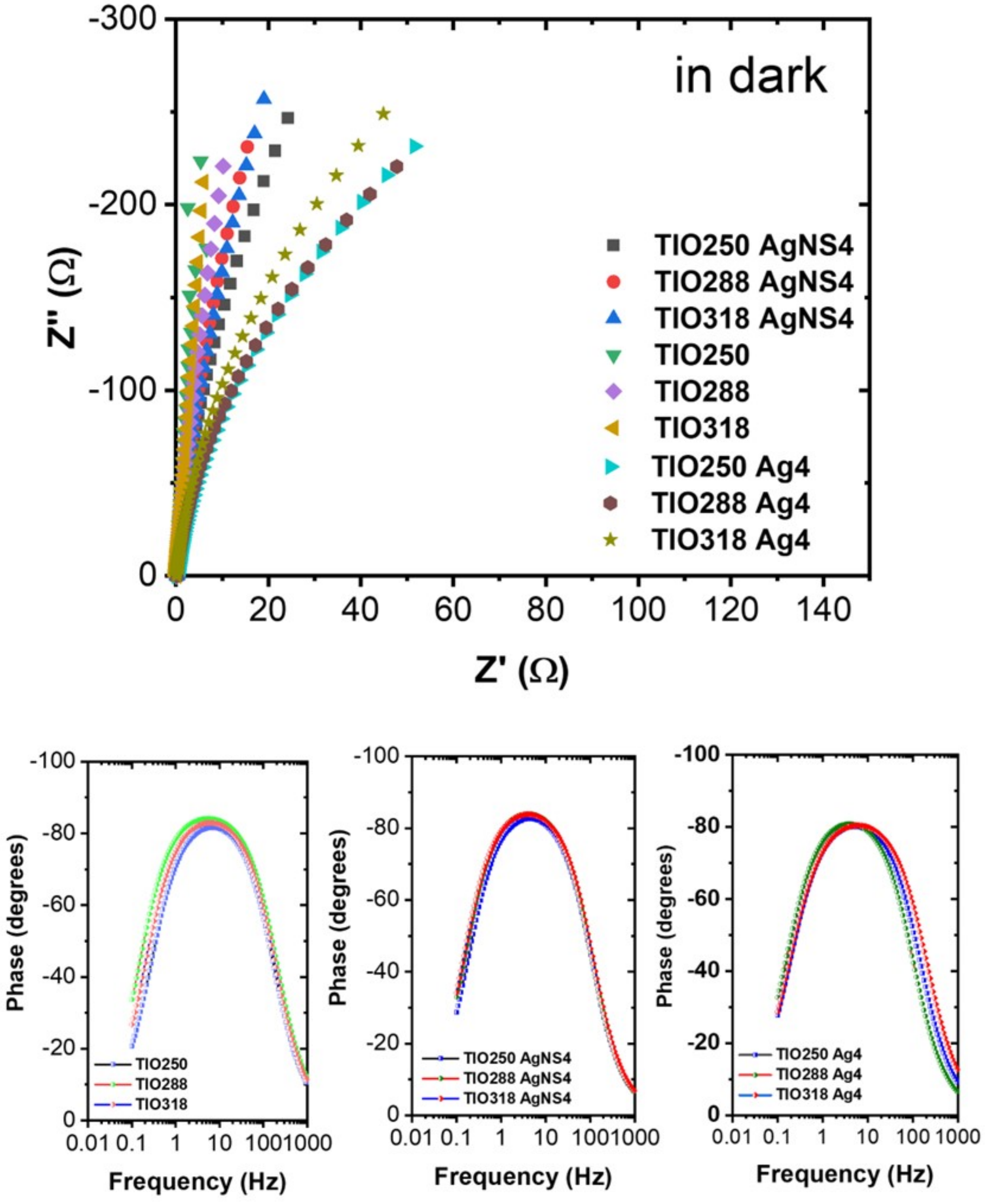

Figure S9. The Nyquist plots of the films in the dark (up), the Bode plots of the film upon the solar light illumination.

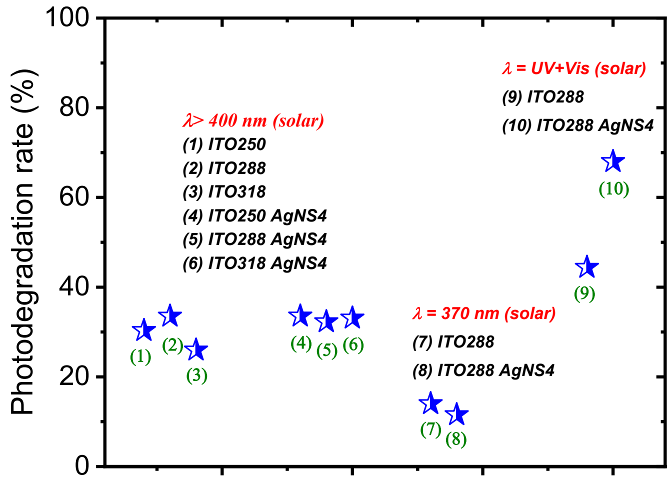

Figure S10. The MB photodegradation rate of different films upon the solar energy light illumination of one sun at different wavelengths.